Anal. Chem. **1996,** *68,* 1798−1804

A Dual Vacuum Chamber Fourier Transform Mass Spectrometer with Rapidly Interchangeable LSIMS, MALDI, and ESI Sources: Initial Results with LSIMS and MALDI

James A. Carroll, Sharron G. Penn, Steven T. Fannin, Jiangyue Wu, Mark T. Cancilla, M. Kirk Green, and Carlito B. Lebrilla*

Department of Chemistry, University of California, Davis, California 95616

A design is presented involving two separate vacuum chambers to provide nearly simultaneous capabilities of liquid secondary ion mass spectrometry (LSIMS), matrix-assisted laser desorption/ionization (MALDI), and electrospray ionization (ESI) in an external source Fourier transform mass spectrometer. The instrument consists of two vacuum chambers, one with five stages of differential pumping for ESI and another with two stages of differential pumping for a combined LSIMS/MALDI source. The chamber dedicated to ESI was formerly a three-stage chamber with LSIMS and electron ionization. Two additional stages were added with the ESI source. LSIMS and MALDI have similar vacuum requirements and were moved to a newly built chamber with two stages of pumping. We present our first results obtained on the new vacuum chamber. Data presented for the MALDI source show that, with only two stages of pumping, and with shorter radio frequency-only quadrupole rods for ion injection, spectra comparable to those obtained on the formerly three-stage instrument can be obtained. Characterization of the MALDI source and data on linear, cyclic, and branched oligosaccharides are given. Finally, the design of the second chamber is proposed as a low-cost prototype for an external source FTMS instrument.

The incorporation of the external source to Fourier transform mass spectrometry (FTMS) has increased its capability both as a research instrument and as an analytical tool. One of the most successful designs involves the use of a quadrupole as an ion guide[1−3] that transports the ions from the source to the analyzer cell. This design has produced ultrahigh mass,[4] ultrahigh resolution,[5,6] and accurate mass determination.[7,8] It is also amenable to several ionization sources, including liquid secondary ionization mass spectrometry (LSIMS), matrix-assisted laser desorption/ionization (MALDI), and electrospray ionization (ESI).

A continuing focus of our research is the development of mass spectrometric techniques for the analysis of oligosaccharides. Given the complex nature of these compounds, it has become necessary to construct instruments with as many different ionization sources as possible. To this end, we set out to develop an FTMS instrument with a variety of ionization sources. Previously, our external source instrument had only electron/chemical ionization (EI/CI) and LSIMS ionization.[9−11] This was subsequently modified to include ESI and MALDI.[12−14] The individual ionization sources are each mounted on a 6 in. flange and are interchangeable by replacing the flange in the source chamber.

It is, however, more desirable to have MALDI, LSIMS, and ESI capabilities nearly simultaneously so that replacing ionization sources is not necessary. Most FTMS employing superconducting magnets have horizontal bores, and one possible design is to incorporate the MALDI and LSIMS source in the chamber on one side of the magnet in the same vacuum chamber and have the ESI on the opposite side. This design would allow the use of each of the three ionization sources without removing the others. However, by using the area on both sides of the analyzer cell, the access to the cell is restricted, prohibiting the use of techniques such as laser photodissociation. It would also require more pumping and an additional ion guide. Furthermore, unless a mechanism is in place to isolate the two chambers, maintenance or repair on one would mean taking down the entire system.

Our approach was to have two separate vacuum systems, with ESI on one side and MALDI/LSIMS on the other (Figure 1). The key is to have a superconducting magnet with magnetic fields that are equivalent on both ends of the bore. With the existing vacuum chamber already resting on a wheeled frame, placing a new chamber on a similarly wheeled frame on the other end allows

(1) Hunt, D. F.; Shabanowitz, J.; Yates, J. R., III; McIver, R. T., Jr.; Hunter, R. L.; Syka, J. E. P. *Anal. Chem.* **1985**, *57*, 2728−33.
(2) Lebrilla, C. B.; Amster, I. J.; McIver, R. T., Jr. *Int. J. Mass Spectrom. Ion Processes* **1989**, *87*, R7−R13.
(3) Lebrilla, C. B.; Wang, D. T.-S.; Hunter, R. L.; McIver, R. T., Jr. *Anal. Chem.* **1990**, *62*, 878−80.
(4) Chen, R.; Cheng, X.; Mitchell, D. W.; Hofstadler, S. A.; Wu, Q.; Rockwood, A. L.; Sherman, M. G.; Smith, R. D. *Anal. Chem.* **1995**, *67*, 1159−63.
(5) Kelleher, N. L.; Senko, M. W.; Little, D. P.; O'Connor, P. B.; McLafferty, F. W. *J. Am. Soc. Mass Spectrom.* **1995**, *6*, 220−221.
(6) McLafferty, F. W. *Acc. Chem. Res.* **1994**, *27*, 379−86.
(7) Li, Y. Z.; McIver, R. T., Jr.; Hunter, R. L. *Anal. Chem.* **1994**, *66*, 2077−83.
(8) McIver, R. T., Jr.; Li, Y. Z.; Hunter, R. L. *Proc. Natl. Acad. Sci. U.S.A.* **1994**, *91*, 4801−5.
(9) McCullough, S. M.; Gard, E.; Lebrilla, C. B. *Int. J. Mass Spectrom. Ion Processes* **1991**, *107*, 91−102.
(10) Carroll, J.; Lebrilla, C. B.; Ngoka, L.; Beggs, C. G. *Anal. Chem.* **1993**, *65*, 1582−7.
(11) Carroll, J. A.; Ngoka, L.; McCullough, S. M.; Gard, E.; Jones, A. D.; Lebrilla, C. B. *Anal. Chem.* **1991**, *63*, 2526−9.
(12) Gard, E.; Carroll, J.; Green, M. K.; Fannin, S. T.; Wu, J.; Camara, E.; Lebrilla, C. B. Presented at the 43rd ASMS Conference on Mass Spectrometry and Allied Topics, Atlanta, GA, May 21−26, 1995.
(13) Green, M. K.; Gard, E.; Camara, E.; Penn, S. G.; Lebrilla, C. B. Presented at the 43rd ASMS Conference on Mass Spectrometry and Allied Topics, Atlanta, GA, May 21−26, 1995.
(14) Fannin, S. T.; Wu, J.; Molinski, T.; Lebrilla, C. B. *Anal. Chem.* **1995**, *67*, 3788−92.

S0003-2700(95)00873-0 CCC: $12.00

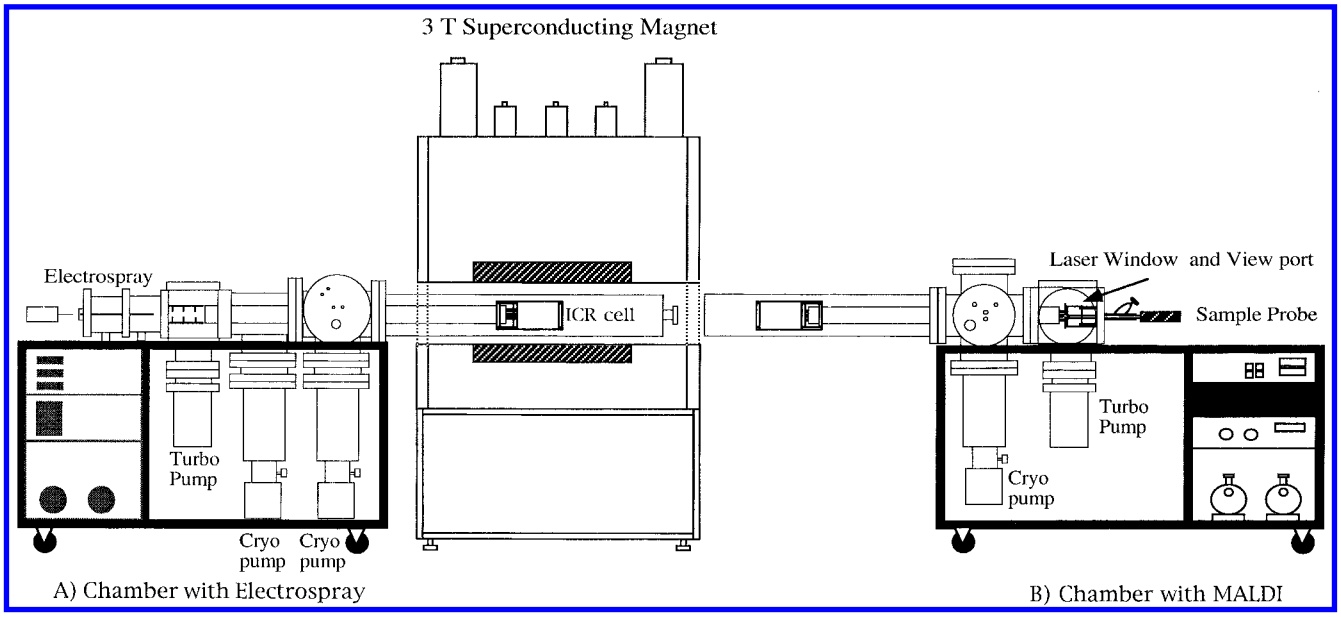

Figure 1. Schematic of the instrument with both vacuum systems consisting of ionization sources, quadrupole ion guide, and analyzer cell. ESI is available on the left chamber, with three stages of differential pumping in the main chamber and two in the source. The right chamber contains the MALDI/LSIMS source. Switching between ESI and MALDI involves rolling one chamber back and the other forward, placing the desired analyzer cell in the homogeneous region of the 3 T superconducting magnet. Switching between MALDI and LSIMS is performed by rotating the probe head 90°.

each cart access to the magnet. The only difference between this design and one utilizing a single main vacuum chamber, with ion sources at both sides of the magnet, is that two analyzer cells are necessary for the two chambers. Otherwise, essentially all pumping and ion guides must still be duplicated on both sides of the magnet. The proposed configuration additionally facilitates the research into different designs for ion optics to be carried out on one chamber while the other is running, thus minimizing overall downtime. The two vacuum chambers sit on separate carts that can be moved into the magnet during the experiments. The pumping requirements will differ for the two systems. ESI requires considerably greater pumping than either LSIMS or MALDI. For this reason, it appeared technically simpler to group the LSIMS and MALDI sources. The current vacuum system consists of three stages of pumping, with a 160 L/s turbo pump on the ionization source cube and two 2000 L/s cryopumps on the transport region. This configuration, along with two other stages of pumping with mechanical pumps, is sufficient to produce and detect electrosprayed ions.[13] Based on our experience with the first vacuum system, it became apparent that the stages of pumping could be decreased and still allow for the use of LSIMS and MALDI. We predicted that it should be possible to construct a chamber with only two stages of differential pumping for the second vacuum chamber.

In this report, we present our approach for a FTMS instrument with LSIMS, MALDI, and ESI that are available nearly simultaneously, utilizing a single data system and a superconducting magnet. This capability is unique to FTMS and would be difficult to implement with other types of mass spectrometers. The first chamber has already been built, so we limit our discussion on the design and construction of a second chamber that is dedicated to MALDI and LSIMS ionization. The results of the electrospray source mounted on the first vacuum chamber have been presented separately.[12,13]

There were several questions about the performance of the new vacuum system that needed to be addressed. First, it was important to determine whether the pumping would be sufficient for FTMS. Our previous design contained at least three stages of differential pumping in the main chamber. Since there are only two stages of pumping in the new design, the ultimate pressure achieved may be insufficient for FTMS analysis, especially when a high-pressure source is used. The pressure in the ICR cell must be kept in the range of 10^{-7} Torr or lower to avoid massive collisional damping of the cyclotron motion, which leads to a decrease in resolution and signal intensity.

The new chamber was also designed with a single set of shorter quadrupole rods. Rods of this length have not been previously reported for injecting externally produced ions into an ICR cell. The shorter length could affect the focusing capabilities of the rods to transport ions effectively. There was also concern whether the trapping efficiency of the ions may be adversely affected, since the rods influence the kinetic energy of the ions.

A third modification to the design was to employ an elongated rather than a cubic analyzer cell. Elongated ICR cells have been shown to have a higher linear range for storing ions by decreasing the space charge effects in the cell.[15] Space charge effects occur when there are too many ions in the cell, leading to excessive Coulombic repulsion between the ions. This has been shown to adversely affect the resolution and mass accuracy by causing dephasing of the ion packet.[15] The elongated design increases the total volume of the cell, so that the space charge limit is not as easily reached. This is especially important for ionization sources operating in the continuous mode, such as EI or LSIMS, in which ions can be continuously collected until the space charge limit is reached. In this way, samples that have poor ionization efficiencies can be detected with improved signal-to-noise ratios simply by increasing the ion loading time. Another feature of the elongated design is that there is less of an effect by the trapping potentials on the motion of the ions in the cell.[15] The presence of trapping potentials is known to result in shifts in the observed

(15) Hunter, R. L.; Sherman, M. G.; McIver, R. T., Jr. *Int. J. Mass Spectrom. Ion Processes* **1983**, *50*, 259−74.

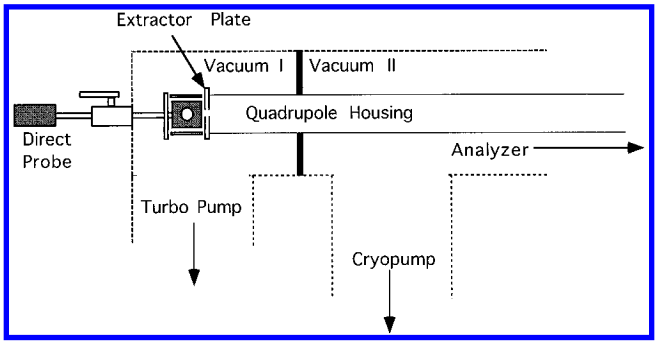

Figure 2. Detail schematics of the source in the MALDI/LSIMS vacuum chamber showing differential pumping. The conductance limit between the two chamber is the extractor plate of the source. The quadrupole housing surrounds the quadrupole rods, effectively placing them in vacuum II.

cyclotron frequency of the ions.[16] Since the ions are less affected by the trapping potentials, frequency shifts are lower in magnitude, and the mass accuracy can be improved relative to a cubic cell.[15]

EXPERIMENTAL SECTION

A schematic of the instrument is shown in Figure 1. To switch from ESI to MALDI, the ESI system is pulled back, and the MALDI/LSIMS system is pushed into position until the analyzer cell of the chamber rests in the homogeneous region of the 3 T superconducting magnet. To convert from MALDI to LSIMS involves only rotation of the probe by 90°. The most noticeable difference between the new vacuum system and the original is the elimination of one stage of vacuum, resulting in considerable savings of time and money. A cryopump and an 8 in. tee have been removed. The gate valve separating the cryopump from the main chamber has also been removed. The new vacuum chamber consists of a 6 in. stainless steel cube to house the ionization source and is connected to a 6 in. six-way cross (MDC, Hayward, CA). A custom-made aluminum tube connected to the six-way cross is used to house the ICR cell, which is centered in the homogeneous region of the superconducting magnet when the instrument is in use. Differential pumping is provided by a 190 L/s turbo molecular pump (Balzers, Hudson, NH) located beneath the source cube and a single 2000 L/s cryopump (APD Cryogenics Inc., Allentown, PA) located beneath the six-way cross.

A single ionization source is used for both MALDI and LSIMS ionization (shown schematically in Figure 2). The ionization source mounts directly on the front flange of the 6 in. cube. The source consists of a stainless steel cube with each plate connected to a separate power supply. The plate that faces the quadrupole rods functions as the extractor. The others serve as repeller and focusing elements. On one focusing plate sits the cesium gun, and the adjacent plate contains a hole that allows the laser beam access to the probe surface. The extractor has an additional function as the constriction between the two differentially pumped chambers. The quadrupole is housed in a solid tube and is fully opened to the lower pressure chamber. The constriction is designed to keep the pressure in the analyzer region sufficiently low for FTMS analysis, even when relatively high pressure ionization sources are in use. There is a trade-off here between high ion throughput and low pressure, with the conductance limit between these two differentially pumped areas being set by the size of the aperture. In this design, 2 mm was the smallest aperture used providing strong ion current. During LSIMS, pressure in the analyzer increased to 5×10^{-8} Torr when a glycerol matrix was applied on the probe tip. Smaller apertures may be used if lower pressures are desired.

Radio frequency-only quadrupole rods are used to transfer the ions from the external source to the analyzer cell. These rods, machined in-house, are similar to the previous design but shorter (0.78 m versus 1.19 m).[9] The rods are powered by a 20 mHz function generator (Model 190, Wavetek, San Diego, CA) and a broadband power amplifier (Model 2100L, Electronic Navigation Industries, Inc., Rochester, NY). A step-up transformer serves to increase the voltage output to the quadrupole rods. The frequency and the amplitude of the applied ac pulse can, therefore, be carefully controlled to maximize the signal of a given mass range. The dc offset is controlled by an external source controller (IonSpec Corp., Irvine, CA). Again, the power supply from the original instrument was used, giving more savings on cost. There is no noticeable difference in capacitance between the two different sets of quadrupole rods, and therefore conditions for successful transportation of ions optimized for the original instrument were found to be also valid for the new instrument.

An elongated ICR cell with dimensions 2 in. × 2 in. × 4 in. is used. The analyzer cell was precision machined out of nonmagnetic 304 stainless steel. MACOR (Corning Glass Works, Corning, NY) machinable ceramic was used to support the cell plates while keeping them electrically isolated. Collar supports and trapping plate supports were machined out of aluminum. Electrical connections to the voltage controller were provided by copper wire covered with insulating sleeves. These were connected to vacuum-sealed electrical feedthroughs in a 10-pin connector welded into a flange on the six-way cross. An electron ionization source is mounted on the rear trapping plate so that ions can be generated in the ICR cell. Machining of all internal parts, such as the ion optics and ICR cell, was carried out in-house at UC Davis.

For MALDI, the instrument contains a pulse valve to allow nitrogen cooling gas to be pulsed into the cell. With 16 Torr of nitrogen behind the pulse valve, a 5 ms pulse raises the pressure in the cell to 1.0×10^{-6} Torr, and after 5 s the pressure falls to mid 10^{-8} Torr, which is sufficient to perform FTMS. Ions produced by LSIMS do not need collision gas for trapping. An LSI (Laser Science, Inc., Newton, MA) 337 N nitrogen laser was mounted directly on the cart for performing MALDI. The beam was pointed directly toward the source and was attenuated by two quartz disks. This produced a laser energy of about 200 μJ per shot with a 3 ns pulse width. The energy was measured under ambient atmosphere with the monitor placed behind the quartz disk and the quartz window.

RESULTS AND DISCUSSION

After the second vacuum chamber was assembled and baked out, the pressure in the analyzer region measured 5×10^{-9} Torr. The pressure did not change significantly when the sample probe was in place, indicating that the differential pumping was suitable for the sample probe assembly. Furthermore, the high mass range (up to m/z 10 000) and the high resolution (210 000 fwhm) discussed below illustrate that performance is not diminished with the shorter rods and only two stages of differential pumping. The external source and the quadrupole rods were evaluated using

(16) Sharp, T. E.; Eyler, J. R.; Li, E. *Int. J. Mass Spectrom. Ion Processes* **1972**, *8*, 237−41.

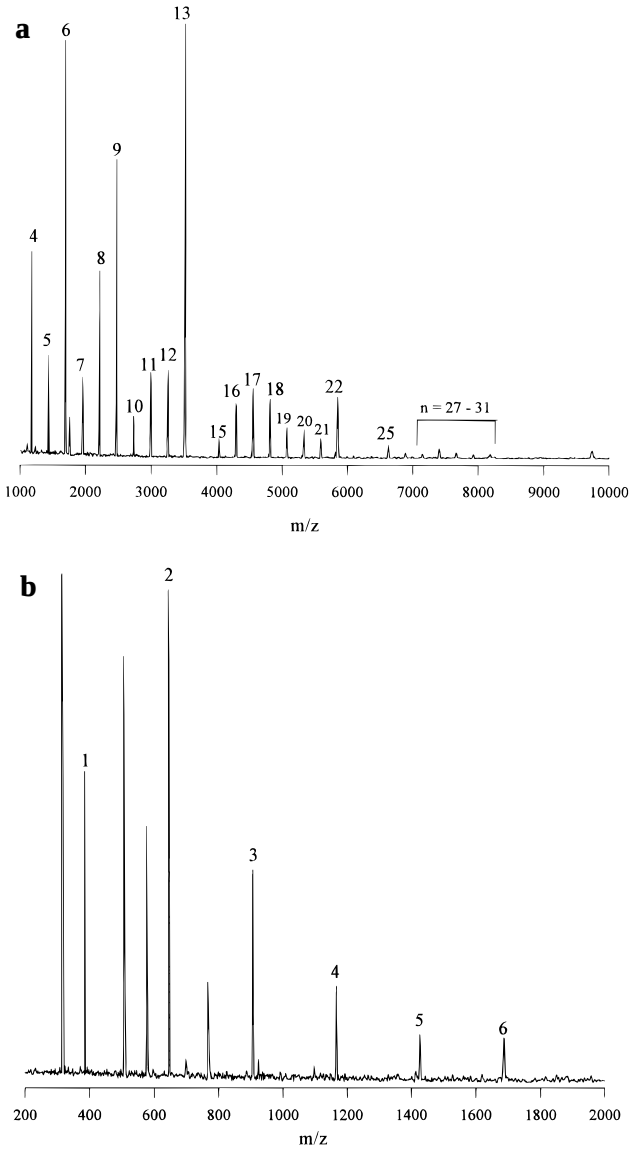

Figure 3. LSIMS spectrum of CsI produced externally in (a) positive ion mode, where the peaks correspond to clusters of the composition $(CsI)_nCs^+$, with the cluster size, *n*, indicated in the spectrum, and (b) negative ion mode, where the peaks correspond to clusters of the composition $(CsI)_nI^-$, with the cluster size, *n*, indicated in the spectrum.

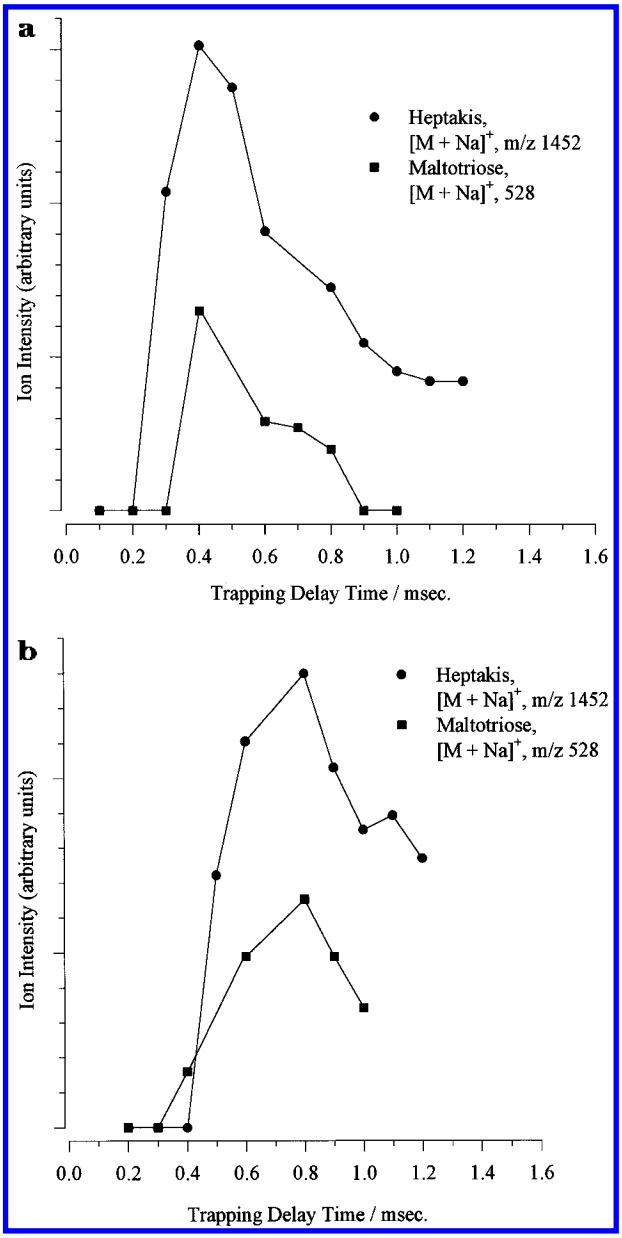

Figure 4. Effect of signal intensity on trapping delay time (a) with extractor plate voltage set at −325 V and quadrupole offset voltage at −50 V and (b) with the quadrupole offset voltage set at −11 V. The quadrupole offset voltage is not mass specific. At −50 V, the maximum signal is obtained with a delay in the trapping delay time of about 0.4 ms. At a lower voltage of −11 V, the optimal trapping delay time is 0.8 ms.

the LSIMS source with CsI placed directly on the sample probe. The ion current on the quadrupole rods was measured to determine the efficiency of ion transmission through the quadrupole rods. The current measured on the quadrupole rods in a typical experiment was 17 nA. To measure this value, the rods were biased (−100 V) to collect all cations entering the ion guide assembly. At times, values as high as 100 nA are measured. On the front trapping plate, the current was measured at 1.7 nA, but could be as high as 30 nA, and ~1.6 nA on the rear trapping plate. Summing the currents on the front and rear trapping plates gives a total (3.3 nA) that is only 20% of the ions entering the quadrupole rods. This apparent ion transport efficiency is low, and we believe that the true value is significantly higher. Primary cations from the source backscatter onto the quadrupole rods, giving an artificially high current reading on the quadrupole rods. Furthermore, the rear trapping plate contains a 90% transmission gold mesh which allows ions to exit.

CsI is also a good compound to study the mass range of the instrument, since CsI forms clusters of the formula $(CsI)_nCs^+$ when subjected to LSIMS, so that the whole range of masses can be investigated. Figure 3a shows the spectra of CsI in the range of m/z 1000−9000. Clusters are observed for the entire mass range. The spectrum is typical of LSIMS spectra of CsI on external source FTMS instruments, with strong signals at clusters with $n = 6$, 9, 13, and 22.[3,9] To date, the largest singly charged ion has m/z 8187, corresponding to a cluster at $n = 31$. These are initial results, and with more tuning and optimization of conditions, the mass range can be increased. The observed mass range, however, is sufficient for much useful analysis, especially with oligosaccharides, which typically fall well within this range. CsI was also used to investigate the anion mode of LSIMS, where the clusters were successfully observed for $(CsI)_nI^-$ (Figure 3b).

The LSIMS system was further tested for the analysis of organic compounds using the tetrapeptide Val-Ala-Ala-Phe in the

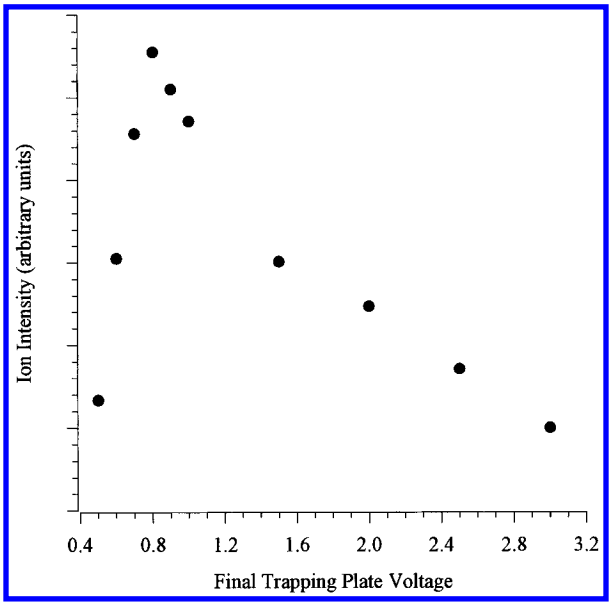

Figure 5. Effect of the trapping plate voltage during ion detection. The drop in intensity is rapid and is due to the rapid decay of transient at moderate trapping voltages.

positive ion mode (not shown). It illustrated that the instrument is useful for analysis of biological compounds and that the performance of this instrument is similar to that of the original instrument.[9] Since previous papers dealing with LSIMS characterization on the original system have been published, no further characterization was carried out. Instead, the instrument was modified to be capable of performing MALDI.

Matrix-Assisted Laser Desorption/Ionization. The ion production and trapping time under LSIMS ionization can be continuously varied. Ion collection can be performed until the space charge limit of the analyzer cell is met. Ions produced by MALDI are formed in a significantly shorter duration. The ions must be trapped immediately after their formation, which is a period lasting only a few milliseconds. Ion trapping is accomplished by raising the rear trapping plate to 10−40 V while maintaining the front trapping plate at 0 V before the laser pulse. After the laser pulse, the front trapping plate is raised to match the rear, and collision gas in the analyzer cell cools the translational energy of the trapped ions. The timing of the pulse sequence in MALDI/FTMS is crucial to the observation of ions.[7,8,17,18] The *trapping delay time* is the time delay from the laser pulse to the raising of the front trapping plate. If the front trapping plate is raised too early, the ions will not have time to traverse the quadrupole rods and consequently will not be able to enter the ICR cell upon arriving. Conversely, if the front trapping plate is raised too late, the ions will enter and exit the cell again. The effect of varying the trapping delay time on the ion intensity of two ions with widely different masses, heptakis-(2,3,6-tri-*O*-methyl)-β-cyclodextrin (MNa^+ *m/z* 1452) and maltotriose (MNa^+ *m/z* 528), was investigated while keeping the extractor voltage and quadrupole offset voltage at −325 and −50 V, respectively—these being typical source conditions (Figure 4a). As shown, the optimum delay times for the sodiated species of both species were identical and found to be 0.4 ms. At shorter

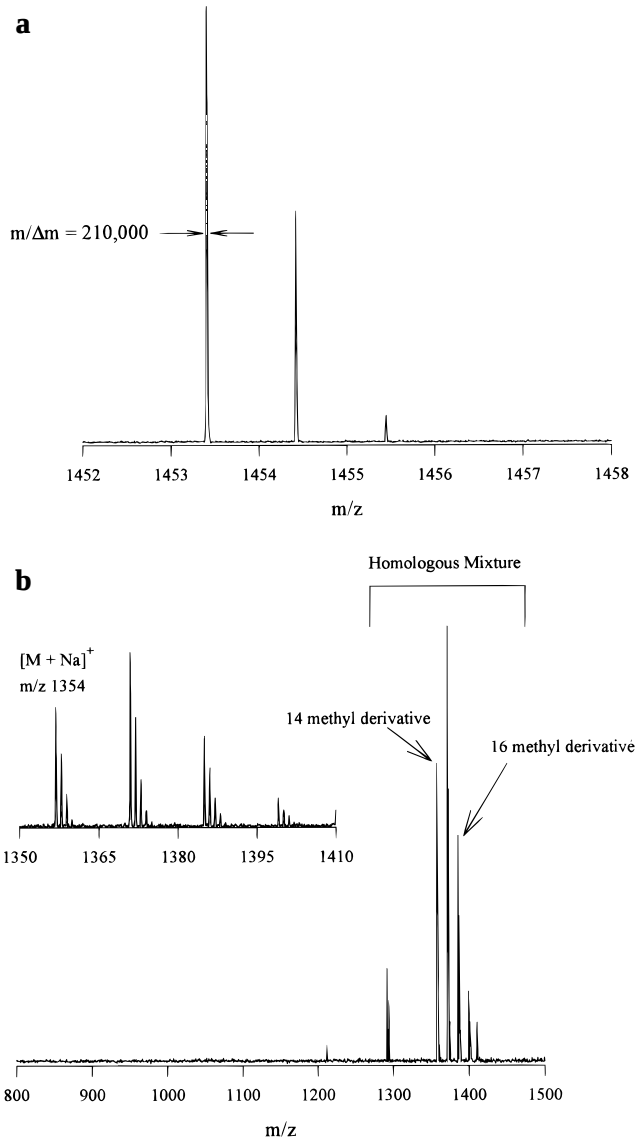

Figure 6. MALDI/FTMS spectra of (a) heptakis(2,3,6-tri-*O*-methyl)-β-cyclodextrin in the quasimolecular ion region and (b) heptakis(2,6-di-*O*-methyl)-β-cyclodextrin. The trimethyl compound is permethylated and shows a single compound. The dimethyl compound is a mixture of compounds with varying amounts of methyl derivatives on the 2 and 6 positions of the glucose units.

times, little or no signal was observed. At longer trapping delay time, the signal was attenuated. There is not a wide variation in the optimal trapping delay time. It is also reassuring that there is not a strong mass dependence on the trapping delay time, at least within the mass range of our interest. We also varied the voltage on the extractor (*extractor plate voltage*) because the *trapping delay time* should be affected by this parameter. We varied the *extractor plate voltage* by as much as 100 V in either direction and found the optimal *trapping delay time* to be only slightly changed (less than 0.05 ms).

Although the extractor plate voltage did not significantly affect the arrival time of the ion, the dc voltage used to bias the quadrupole rod assembly showed direct dependency. Voltage is applied to the quadrupole rod (*quadrupole offset voltage*) to transport the ion through. This voltage is felt by the ion as it nears the aperture on the extractor plate. Figure 4b shows the total ion intensity as a function of *trapping delay time* with the *quadrupole offset voltage* set at −11 V for both heptakis(2,3,6-tri-

(17) Castoro, J. A.; Koster, C.; Wilkins, C. *Rapid Commun. Mass Spectrom.* **1992**, *6*, 239−41.
(18) Stemmler, E. A.; Hettich, R. L.; Hurst, G. B.; Buchanan, M. V. *Rapid Commun. Mass Spectrom.* **1993**, *7*, 828−36.

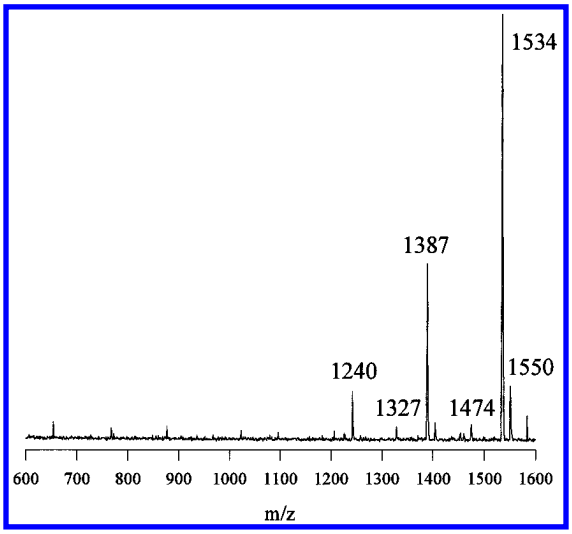

Figure 7. MALDI/FTMS mass spectrum of a branched saccharide trifucosyllacto-*N*-hexaose found in human milk. Fragmentation is abundant, with the loss of the fucosyl group as the most dominant product.

O-methyl)-*β*-cyclodextrin and maltotriose. Under these conditions, the optimum delay time increased to 0.8 ms for both ionic species, with virtually no ions being trapped at 0.4 ms delay. For tuning, several sets of conditions are optimal for obtaining intense signals. At the moment, it is easier to fix the *trapping delay time* and vary the *quadrupole offset voltage* to optimize the signal. The signal is highly sensitive to the optimum *trapping delay time*, making it difficult to find without laborious experimentation. In comparison, the signal is less sensitive to the *quadrupole offset voltage*.

Another important parameter is the trapping plate voltage during ion detection. While the trapping plate voltage is kept at 10−40 V during collection and cooling of the ion population, it is ramped to a lower voltage at the time of detection. Figure 5 shows the effect of the final trapping plate voltage, the value during detection, on the ion intensity of heptakis(2,3,6-tri-*O*-methyl)-*β*-cyclodextrin when 256*K* data points are transformed. It would appear that a trapping plate voltage of between 0.5 and 1.0 V gives the optimum trapping conditions. There are two effects operating to produce this behavior. At lower voltages, ion loss is high, resulting in attenuation of the signal. At higher voltages, the transient decays much more rapidly, again decreasing the signal intensity. When only the first 8*K* data points were transformed, the decrease above 1.0 V was not observed. Minimizing the trapping plate voltages is also important for obtaining exact masses for elemental composition.[14]

Figure 6a shows the molecular ion region of heptakis(2,3,6-tri-*O*-methyl)-*β*-cyclodextrin (**1**). This is a fully methylated cyclic oligosaccharide. ^{13}C Isotopic resolution is achieved with a resolution of 210 000 (fwhm), and it is noteworthy that the quasimolecular ion is a sodium adduct, although no doping had been carried out. The sodiated species is always the most abundant species in the MALDI/FTMS of oligosaccharides. No other ions are observed in this spectrum. The alkali metal ions are thought to be ubiquitous in the sample. A sample of partially methylated heptakis(2,6-di-*O*-methyl)-*β*-cyclodextrin which contains various numbers of methyl derivatives was also analyzed. The spectrum of the mixture (Figure 6b) shows again that isotopic resolution is achieved for all the components and that sodium adduction is also seen. This is a very encouraging result, since it demonstrates that mixture analysis of oligosaccharides is possible.

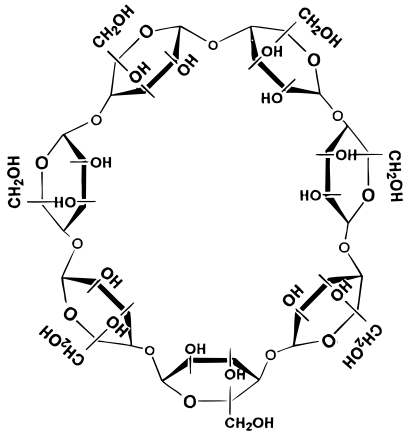

1

Figure 7 shows the mass spectrum of trifucosyllacto-*N*-hexaose (**2**), a branched oligosaccharide found in human milk. Consider-

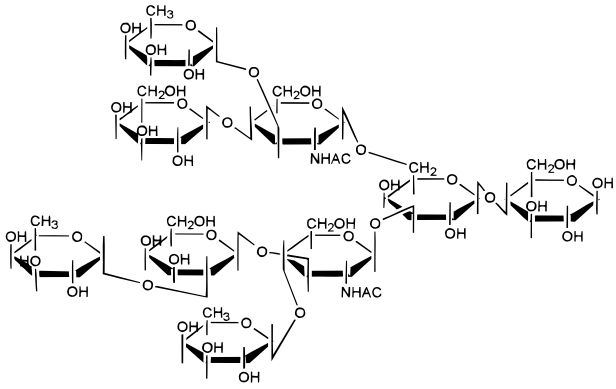

2

able fragmentation is observed compared to MALDI/TOF spectra of similar compounds that show only quasimolecular ion.[19] Similar fragmentation is observed only with the use of postsource decay, which applies harsh conditions to the ionization to produce fragmentation.[20,21] Once again, sodiated species are observed (*m/z* 1534), along with a small amount of potassiated species (*m/z* 1550). The peaks at *m/z* 1387 and 1240 are due to the loss of one and two fucose subunits, respectively. The loss of fucosyl groups as the major mode of fragmentation is intriguing. All are on the nonreducing end of the sugar. A fourth sugar, glucose, is also on the nonreducing end but does not dissociate. Cross-ring cleavage is also observed, albeit only from the reducing end. The ^{0,2}A cleavage (according to the Domon and Costello formalism,[22] observed as *m/z* 1474 and 1327) is consistent with the 1−4 linkage of the reducing sugar.[10]

The key advantage to trapping ions produced by MALDI in FTMS is that collisionally induced dissociation (CID) can be performed on the ions. To further assess the capability of the

(19) Stahl, B.; Thurl, S.; Zeng, J. R.; Karas, M.; Hillenkamp, F.; Steup, M.; Sawatzi, G. *Anal. Biochem*. **1994**, *223*, 218−26.
(20) Spengler, B.; Kirsch, D.; Kaufmann, R.; Lemoine, J. *J. Mass Spectrom*. **1995**, *30*, 782−7.
(21) Spengler, B.; Kirsch, D.; Kaufmann, R.; Lemoine, J. *Org. Mass Spectrom*. **1994**, *29*, 782−7.
(22) Domon, B.; Costello, C. E. *Glycoconjugate J.* **1988**, *5*, 397−409.

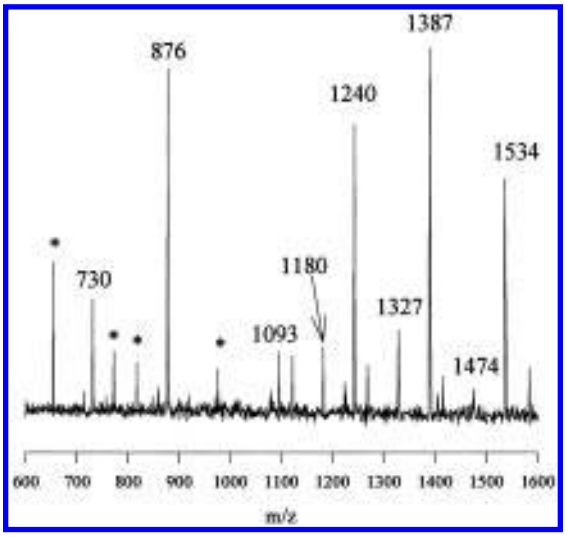

Figure 8. Collisionally induced dissociation spectrum of sodiated trifucosyllacto-*N*-hexaose produced by MALDI. Abundant fragments are observed, providing information on sequence and linkage. The peaks with asterisks are due to electronic noise from the laser. Work is currently under way to eliminate the noise.

instrument, CID of trifucosyllacto-*N*-hexaose was performed. Figure 8 shows the CID spectrum of the sodiated species. The advantage of performing CID on the sodiated species is that linkage information due to cross-ring cleavage is also obtained, in addition to molecular weight and sequence information. Protonated species would provide only the latter information. The CID experiment involved isolating the desired ion (MNa^+, m/z 1534) and exciting the ion at its cyclotron frequency for 0.25 ms with 24 V_{p-p} amplitude. As can be seen in Figure 8, CID causes extensive fragmentation compared with MALDI fragmentation alone (Figure 7). There are several new fragments, and many of those observed with only MALDI are considerably enhanced. Important features in the CID spectrum are a peak at m/z 1093 corresponding to the loss of a third fucose unit, and a further $^{0,2}A$ fragment at m/z 1180 corresponding to the loss of 60 from the m/z 1240 ion. While the pseudomolecular ion MNa^+ (m/z 1534) was the predominant feature in Figure 7, the predominant ion in the CID spectra (Figure 8) is now the $Y_{2\beta}$ fragment at m/z 876. In addition, a new fragment, not seen in Figure 7, at m/z 730 is observed in the CID spectrum, this being the $Y_{3\alpha}$ fragment. These two fragments (m/z 876 and 730) result from fragmentation of the two major antennae of trifucosyllacto-*N*-hexaose. Figure 8, therefore, demonstrates the power of CID in obtaining sequence *and* structural information on highly branched oligosaccharides. Further work is in progress on extending these methods to other branched oligosaccharides of biological importance.

CONCLUSIONS

The new chamber has met the design goals of relatively low cost, versatility of ionization methods, and high performance. Both LSIMS and MALDI sources provide high-quality spectra comparable to spectra obtained from other, more expensive designs. The decrease in pumping has not adversely affected the performance of the instrument. This instrument shows promise for the analysis of biological molecules.

The cost of the new chamber is estimated to add an additional 15% to the entire cost of instrument. Compared to the first chamber, its cost is less than 50%. However, the second chamber offers great versatility and allows the analysis of most types of biological compounds. The design of the second chamber will also serve as a prototype for a low-cost external source instrument with a quadrupole ion guide. For us, it offers the opportunity for direct comparison of the energetics of ion formation associated with LSIMS, MALDI, and ESI.

ACKNOWLEDGMENT

Funds provided by the National Institute of General Medical Sciences, NIH (Grant GM49077-01), and the National Science Foundation (Grant CHE 9310092) are gratefully acknowledged. We thank the reviewers for their helpful comments.

Received for review August 24, 1995. Accepted March 12, 1996.[⊗]

AC950873P

[⊗] Abstract published in *Advance ACS Abstracts,* April 15, 1996.